Optical-Model Analysis of 15-MeV Deuteron Elastic Scattering

C. M. PEREY* AND F. G. PEREY
Neutron Physics Division, Oak Ridge National Laboratory,† Oak Ridge, Tennessee
(Received 12 December 1963)

An optical-model analysis is made of deuteron elastic scattering from several nuclei for a deuteron bombarding energy of 15 MeV. The trend of the optical-potential parameters to vary smoothly as a function of mass number is found to be in essential agreement with that obtained in a previous analysis. Numerical values of the parameters are given and should be of help in generating wave functions for distorted-wave analysis of deuteron reactions at 15 MeV.

I. INTRODUCTION

IN a previous paper[1] (hereafter referred to as paper 1) we reported on an optical-model analysis of deuteron elastic scattering from many nuclei for deuteron bombarding energies between 11 and 27 MeV. It was shown that, with few exceptions, it is possible to reproduce the data quite well with *several families* of optical potentials whose parameters vary smoothly as a function of mass number and energy. Soon after the analysis of paper 1 was completed, Jolly *et al.*[2] reported angular-distribution measurements for the elastic scattering of 15-MeV deuterons from several elements not included in our analysis. Since one of the purposes of the previous analysis was to obtain optical-model parameters that would be useful in distorted-wave Born-approximation (DWBA) calculations of stripping and inelastic scattering, and in view of the large amount of such data available at 15 MeV, we decided to extend the analysis of paper 1 to the new data.

II. METHOD OF ANALYSIS

Only the main points of the method of analysis are given here, since the procedure is similar to that used in paper 1, which is assumed to be familiar to the reader.

The optical-model potential used is defined as

$$\text{real part:} \quad -V_S f(r,r_{0S},a_S),$$

$$\text{imaginary part:} \quad 4a_I W_D \frac{d}{dr} f(r,r_{0I},a_I).$$

The imaginary part of the potential is of the surface type, with the factor $4a_I$ introduced so that the surface form-factor $4a_I df/dr$ has unity for its maximum value. The function $f(r,r_0,a)$ is the usual Woods-Saxon form factor:

$$f(r,r_0,a)=\{1+\exp[(r-r_0A^{1/3})/a]\}^{-1},$$

where A is the atomic mass of the nucleus in amu.

The Coulomb potential used is

$$Ze^2/2R_C[3-(r^2/R_C^2)] \quad \text{for} \quad r\leqq R_C,$$

and

$$Ze^2/r \quad \text{for} \quad r>R_C,$$

which is that produced by a uniform charge distribution of radius R_C. The results of the analysis are not very sensitive to the value of R_C, which was therefore kept fixed at $1.3A^{1/3}$ F.

The numerical values of the experimental differential cross section $\sigma_{\text{exp}}(\theta_i)$ are used in an automatic parameter search routine incorporated in the optical-model program. The parameters of the model are varied to obtain a minimum value of χ^2, defined as

$$\chi^2=\frac{1}{N}\sum_{i=1}^{N}\left[\frac{\sigma_{\text{th}}(\theta_i)-\sigma_{\text{exp}}(\theta_i)}{\Delta\sigma_{\text{exp}}(\theta_i)}\right]^2,$$

where $\sigma_{\text{th}}(\theta_i)$ are the theoretical differential cross sections, and $\Delta\sigma_{\text{exp}}(\theta_i)$ the experimental errors.

Jolly *et al.*[2] do not quote an experimental error but state that their cross sections are the average of several independent measurements and that the statistics on the counts recorded in the elastic-scattering peak are better than 1%. In view of the scatter of the points from a smooth line drawn through the data, we assigned an error of 5% to all the data except those for Ni^{58}, Zr, Sn^{120}, and Au. The data for these four elements, which were kindly made available by Jolly *et al.* prior to their publication and were included in our analysis in paper 1, were assigned errors of 10% for angles less than 90° and errors of 15% for larger angles. In order to present a complete analysis of the data of Jolly *et al.* in one paper, the results of the analysis for these four elements are included here but their χ^2 values are now multiplied by 4 to permit an easier comparison with the quality of fits to the data for the other elements. Since we experienced some difficulty during the analysis with the data for Rh and Pd, we had to renormalize them by 0.7 and 0.82, respectively. (This point is more fully treated under "Discussion.") The renormalized data were used in the analysis discussed below.

III. BEST FIT TO THE DATA: SET a

In paper 1 one family of potentials used to analyze all the data was designated as "set a" and is characterized by a given value for the product $V_S r_{0S}^2$. Many other discrete families of potentials can be found, but since,

* Consultant.
† Operated by Union Carbide Corporation for the U. S. Atomic Energy Commission.
[1] C. M. Perey and F. G. Perey, Phys. Rev. **132**, 755 (1963).
[2] R. K. Jolly, E. K. Lin, and B. L. Cohen, Phys. Rev. **130**, 2391 (1963).

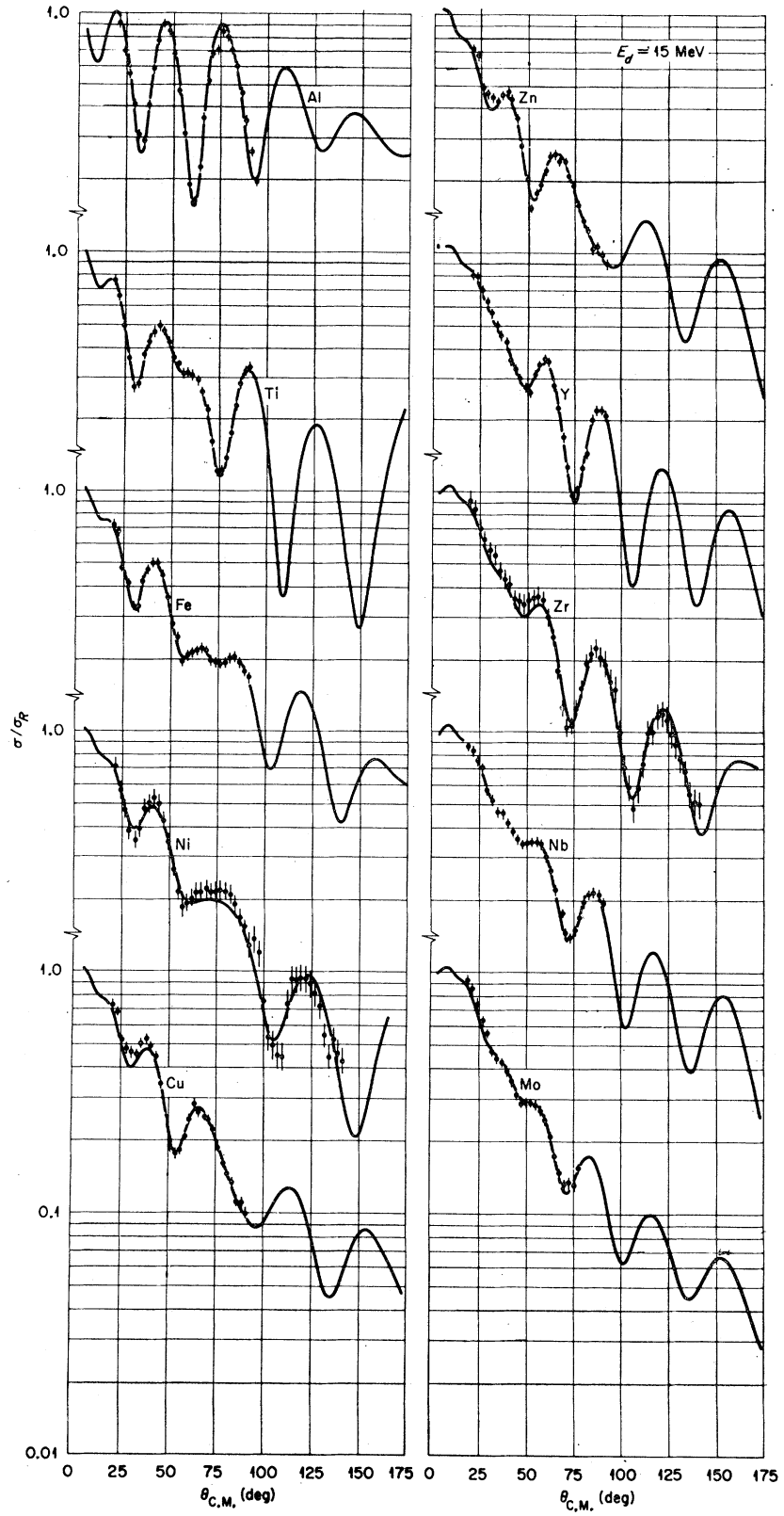

FIG. 1. Comparison of the data of Jolly *et al.* (Ref. 2) for elements up to Mo with the curves obtained with the parameters given in Table I. All the parameters of the potentials were adjusted by the code for a minimum value of χ^2.

TABLE I. Results of the search code fitting all the 15-MeV data by allowing the six parameters to be adjusted for a minimum χ^2 value (set a).

Element	V_S (MeV)	r_{0S} (F)	a_S (F)	W_D (MeV)	r_{0I} (F)	a_I (F)	σ_R (mb)	χ^2 (F)
Al	39.0	1.300[g]	0.883	22.50	1.480	0.535	1281	3.5
Ti	52.4	1.158	0.854	11.56	1.448	0.687	1504	0.31
Ti[a]	35.8	1.453	0.721	13.66	1.414	0.609	1472	6.2
Fe	59.4	1.105	0.884	13.40	1.389	0.712	1532	0.68
Fe[a]	30.4	1.616	0.679	19.47	1.498	0.432	1528	7.7
Fe[a,b]	51.9	1.185	0.873	13.23	1.420	0.703	1576	1.6
Ni^{58}	76.1	0.931	0.840	11.15	1.284	0.850	1484	4.0
Cu	83.5	0.918	0.952	13.73	1.336	0.730	1503	1.7
Cu[a]	73.3	0.982	1.118	14.70	1.409	0.710	1722	5.2
Cu[a,c]	64.9	1.080	0.976	13.52	1.459	0.702	1696	1.3
Zn	95.1	0.840	1.054	13.86	1.371	0.714	1560	1.1
Y	52.2	1.321	0.706	14.15	1.330	0.616	1452	0.71
Zr	68.1	1.098	0.911	11.66	1.404	0.682	1572	2.5
Nb	56.9	1.271	0.731	13.56	1.324	0.672	1467	0.26
Mo	68.1	1.119	0.927	14.60[g]	1.359	0.688	1591	0.82
Rh[d]	71.3	1.146	0.911	16.16	1.383	0.700	1660	2.0
Rh[a]	78.5	0.996	1.036	12.02	1.453	0.877	2028	1.9
Pd	118.9	0.845	0.693	12.58	0.970	1.026	1265	1.6
Pd[e]	76.3	1.032	0.974	14.80	1.353	0.771	1678	1.1
Pd[a]	68.1	1.114	0.864	9.97	1.470	0.908	2035	2.7
Ag	44.9	1.471	0.631	25.28	1.368	0.510	1518	0.79
Cd	77.6	1.036	0.931	15.22	1.324	0.758	1584	0.55
In	54.1	1.268	0.715	15.27	1.236	0.723	1417	0.46
Sn[a]	77.5	0.994	1.160	12.54	1.535	0.771	2061	2.3
Sn^{120}	75.3	1.104	0.688	10.29	1.247	0.940	1582	2.6
Er	83.5	0.961	1.159	17.78	1.363	0.660	1456	0.25
Yb	50.2	1.376	0.705	17.93	1.272	0.730	1450	0.27
Ta	74.5	1.283	0.796	18.64	1.350	0.744	1527	0.45
Ta[a]	49.3	1.469	0.669	24.69	1.437	0.540	1473	2.3
W	114.5	0.936	1.112	25.67	1.330	0.593	1262	0.22
Pt	55.3	1.445	0.512	14.13	1.094	1.177	1608	0.10
Au	86.7	1.054	0.789	6.93	1.370[g]	1.032	1595	0.28
Au[a]	89.7	1.011	1.113	13.09	1.455	0.693	1477	1.5
Pb	127.6	0.895	0.919	8.06	1.055	1.267	1336	3.9
Pb[f]	65.1	1.291	0.805	14.91	1.381	0.656	1302	0.62
Pb[a]	93.4	0.986	1.184	12.43	1.484	0.621	1406	1.7

[a] Cindro and Wall data.
[b] Data renormalized by 1.6.
[c] Data renormalized by 1.5.
[d] Data renormalized by 0.7.
[e] Data renormalized by 0.82.
[f] Parameters obtained by fitting the data up to 90°.
[g] Value of parameter not adjusted by code.

as was shown in paper 1, all the different potentials give almost identical differential cross sections, we did not think it worthwhile at this stage to exhibit them for the 15-MeV data and therefore used only set a.

The set of potentials of family a is obtained by allowing the search code to fit the data by adjusting the six parameters of the model. The starting values of the parameters bias the search code to find local minima in the region of parameter space spanned by the particular family of potentials being sought.

The parameters found for set a are given for all the data in Table I, and the resulting fits to the data for elements up to Mo are shown in Fig. 1. For the heavier elements the diffraction pattern are very weak up to 90°, and consequently the fits are in general indistinguishable from a smooth line drawn through the data points, as indicated by the low value of χ^2. For these new data, as well as for the more extensive survey of paper 1, the scatter of the values of the parameters so obtained is fairly large. The only general trend indicated in Table I is that the real radius parameter r_{0S} is small, often smaller than 1 F, whereas the imaginary radius parameter r_{0I} is much larger, in almost all the cases greater than 1.30 F.

IV. SYSTEMATIC ANALYSIS: SET c

In paper 1 the angular distributions were fitted for each of four sets of geometrical parameters by allowing the search code to adjust V_S and W_D for the lowest χ^2 values for each element. Since all the sets of potentials gave similar fits to the data, in this extended analysis we investigated only set c, which has the following parameter values:

$$r_{0S}=1.30\text{ F} \qquad a_S=0.79\text{ F}$$
$$r_{0I}=1.37\text{ F} \qquad a_I=0.67\text{ F}.$$

Table II gives the well-depth values that yielded the minimum χ^2 values, and Figs. 2 and 3 show the resulting fits to the data. In general, the fits to the data are

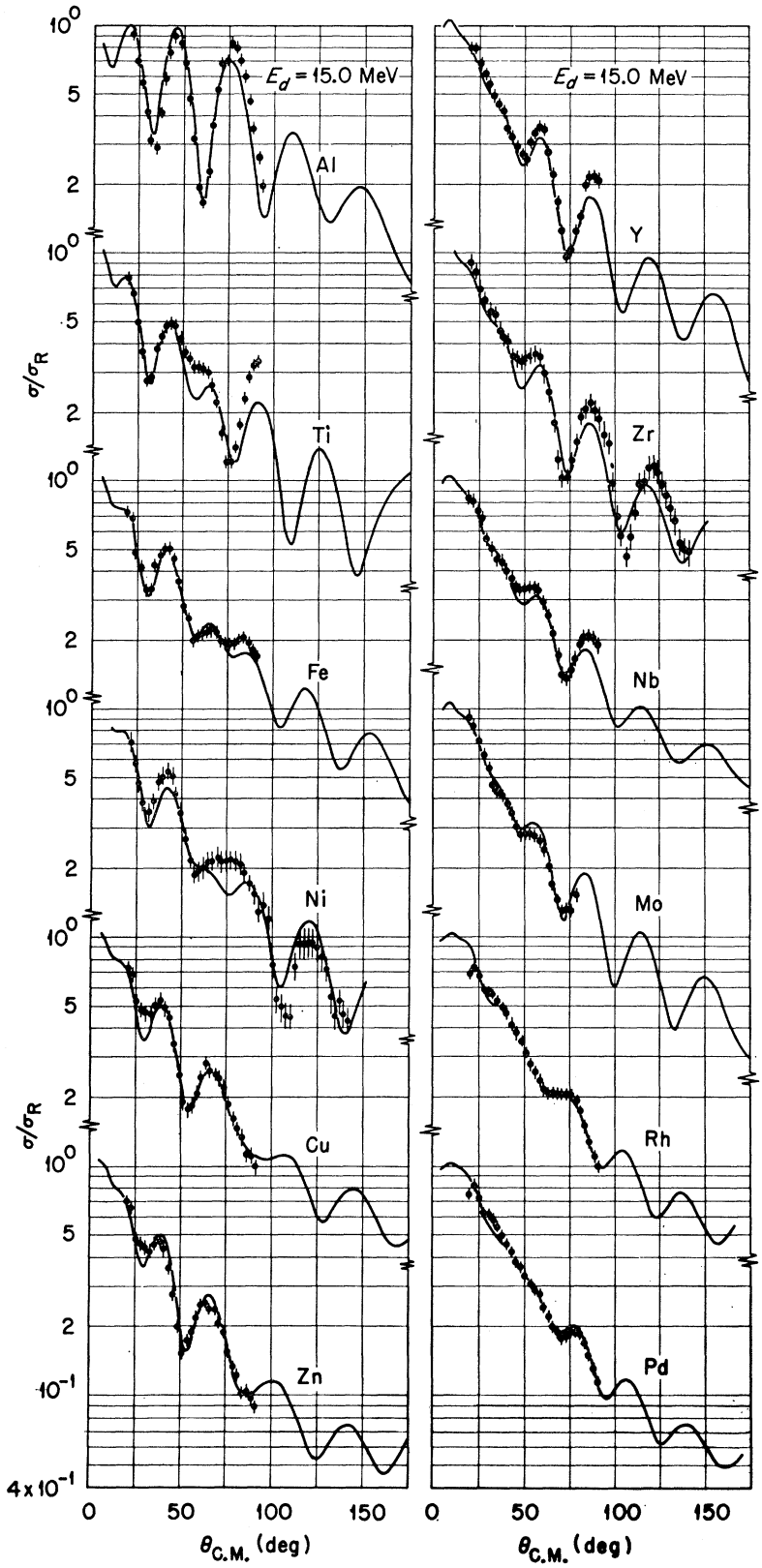

FIG. 2. Comparison of the data of Jolly *et al.* (Ref. 2) for elements through Pd with the curves obtained with the parameters given in Table II. The data for Rh and Pd are renormalized by 0.7 and 0.82, respectively. The geometrical parameters are the same for all elements; their values are given in Sec. IV. For each angular distribution, the well-depths V_S and W_D are adjusted to give the lowest value of χ^2.

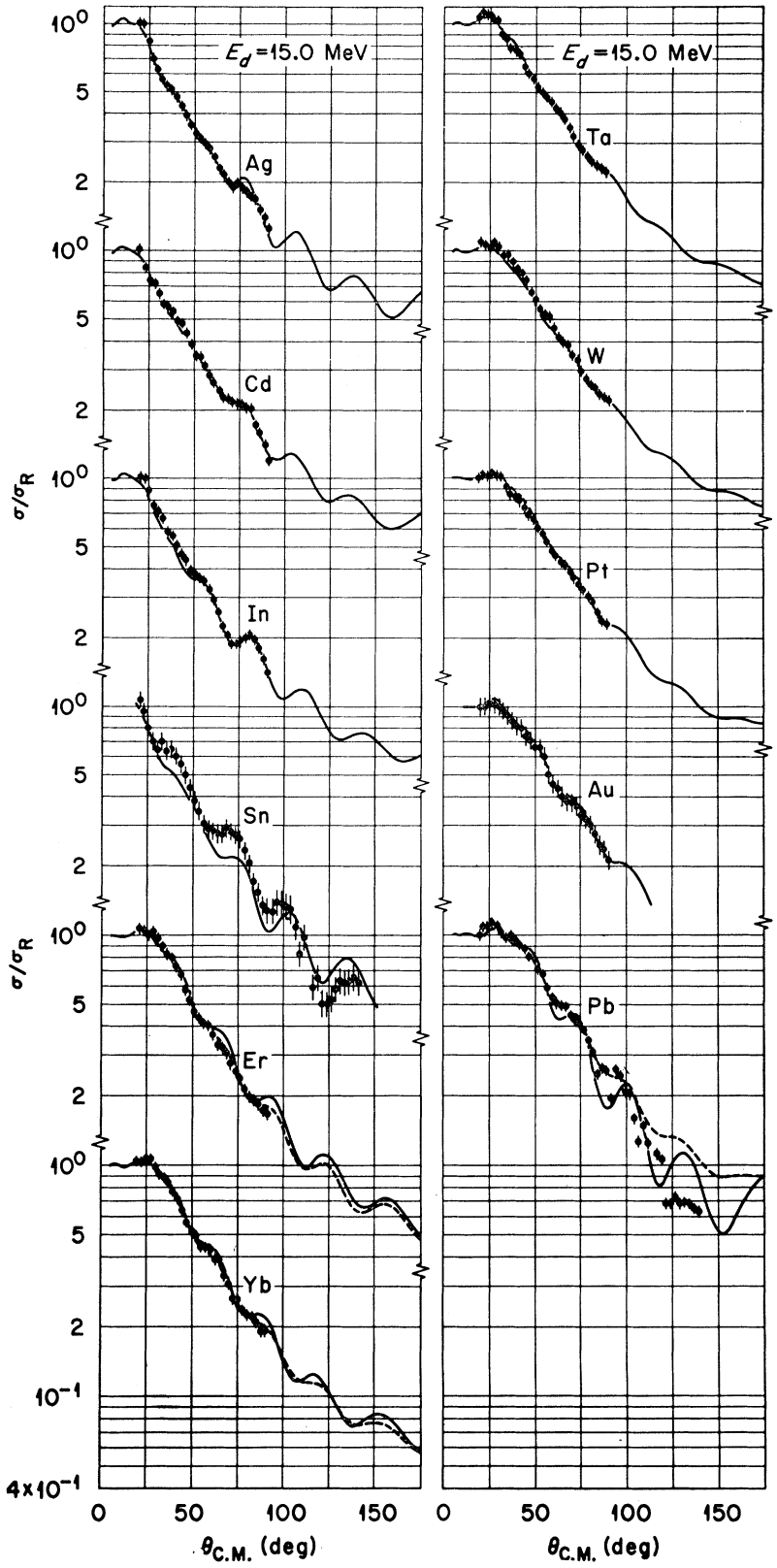

FIG. 3. Comparison of the data of Jolly *et al.* (Ref. 2) for elements above Pd with the curves obtained with the parameters given in Table II. The geometrical parameters are the same for all elements; their values are given in Sec. IV. For each angular distribution, the well-depths V_S and W_D are adjusted to give the lowest χ^2 value. The dashed curves for Er and Yb are obtained from parameters of the next family of deeper potentials as explained in Sec. V. The dashed curve for Pb is the fit obtained from a search on V_S and W_D made with data for angles smaller than 90°.

satisfactory. The values of V_S and W_D are plotted in Fig. 4 as a function of $Z/A^{1/3}$, together with those obtained in paper 1 from the analysis of the 15-MeV data of Cindro and Wall[3] for nine elements. The line showing the trend of V_S was obtained from the analysis of Cindro and Wall's data in paper 1.

The two sets of data are compared in the following section, and the large departure of some of the real well depths from the general trend is discussed.

V. DISCUSSION

Comparison of the Data

Figure 5 compares the data for the nine elements studied by Cindro and Wall with the data obtained by Jolly *et al.* when they remeasured these elements. Also shown are the fits to the data obtained by using the set C parameters. With the exception of Au and Ta, the two sets of data are quite different, much outside the combined experimental error. For Ti there is general agreement as to the amplitude of the oscillations and their angular positions except in the range 35 to 60°. For Fe and Cu the two sets of data are in fair agreement up to 30°, but differ markedly for larger angles. If the data of Cindro and Wall for angles greater than 30° are multiplied by 1.6 for Fe and 1.5 for Cu, there is good agreement with the data of Jolly *et al.* There is no indication, however, that such a correction could be justified on the basis of their experimental technique, but even the optical-model fits to their original data, at least up to 75°, seem to require this normalization.

Similar disagreement exists between the two sets of data for Rh and Pd, and it is impossible for the optical model to fit the data of Jolly *et al.* up to 50° because the calculated differential cross sections up to this angle are fairly insensitive to the value of the well depth once the geometrical parameters are fixed at some reasonable values, such as those of set c. When we multiply their data for Rh by 0.7 and for Pd by 0.82, good agreement between the two sets of data and between the data and the optical-model curves is obtained. Since the normalization of the data of Jolly *et al.* was obtained in a separate experiment, it seems that the above correction could be justified.

For Sn there is a large discrepancy between the two sets of data up to 90°; however, the optical-model fits to both sets agree with each other remarkably well in this angular region and for angles greater than 75° tend to favor the data of Cindro and Wall. The agreement

TABLE II. Results of the search code fitting all the 15-MeV data by allowing the well-depths V_S and W_D to be adjusted for a minimum χ^2 value while the geometrical parameters are kept fixed.

Element	V_S (MeV)	W_D (MeV)	σ_R (mb)	χ^2
Al	36.8	18.3	1308	16
Ti	43.8	14.8	1478	13
Ti[a]	43.6	13.4	1462	9.2
Fe	44.9	16.0	1515	2.3
Fe[a]	45.4	12.1	1477	38
Fe[a,b]	44.5	15.1	1505	3.4
Ni^{58}	43.3	15.6	1468	10
Cu	47.4	15.7	1556	3.9
Cu[a]	49.7	13.5	1543	37
Cu[a,c]	48.7	15.6	1560	5.0
Zn	48.9	15.1	1553	4.4
Y	51.6	14.3	1602	4.0
Zr	51.4	14.6	1600	8.4
Nb	52.0	16.9	1614	3.2
Mo	53.4	14.6	1604	2.5
Rh	52.9	28.6	1676	17
Rh[d]	58.6	17.3	1632	2.0
Rh[a]	57.6	14.6	1608	19
Pd	51.6	22.6	1645	6.9
Pd[e]	54.4	16.8	1620	1.4
Pd[a]	56.9	14.4	1612	13
Ag	55.4	17.3	1612	1.3
Cd	54.2	18.8	1630	0.86
In	49.4	16.4	1587	1.5
Sn[a]	56.2	14.9	1612	8.5
Sn^{120}	54.2	15.4	1619	8.8
Er	53.8	12.6	1429	3.1
	74.0	17.7	1540	0.79
Yb	56.0	13.4	1425	1.6
	74.4	19.2	1527	0.45
Ta	72.9	20.8	1483	0.55
Ta[a]	61.9	22.8	1453	2.7
W	69.4	19.8	1458	0.72
Pt	66.1	17.1	1378	0.79
Au	63.6	17.2	1335	3.8
Au[a]	62.8	17.2	1345	2.9
Pb	64.9	9.5	1270	23
Pb[f]	64.6	14.8	1305	0.62
Pb[a]	62.4	19.0	1316	6.4

[a] Cindro and Wall data.
[b] Data renormalized by 1.6.
[c] Data renormalized by 1.5.
[d] Data renormalized by 0.7.
[e] Data renormalized by 0.82.
[f] Parameters obtained by fitting the data up to 90°.

[3] N. Cindro and N. S. Wall, Phys. Rev. **119**, 1340 (1960).

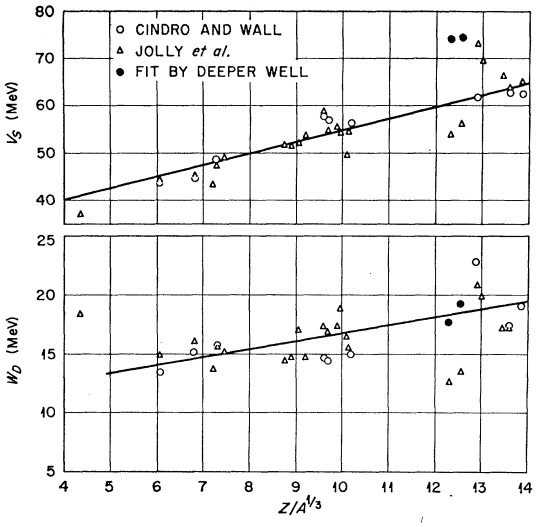

FIG. 4. The real well-depths V_S and the imaginary well-depths W_D, as functions of the Coulomb-parameter $Z/A^{1/3}$ for the fits to the data of Jolly *et al.* (Ref. 2) and Cindro and Wall (Ref. 3). The potentials were obtained by adjusting V_S and W_D for the lowest χ^2 value when the geometrical parameters are kept fixed at the values given in Sec. IV. The numerical values of the well depths are given in Table II.

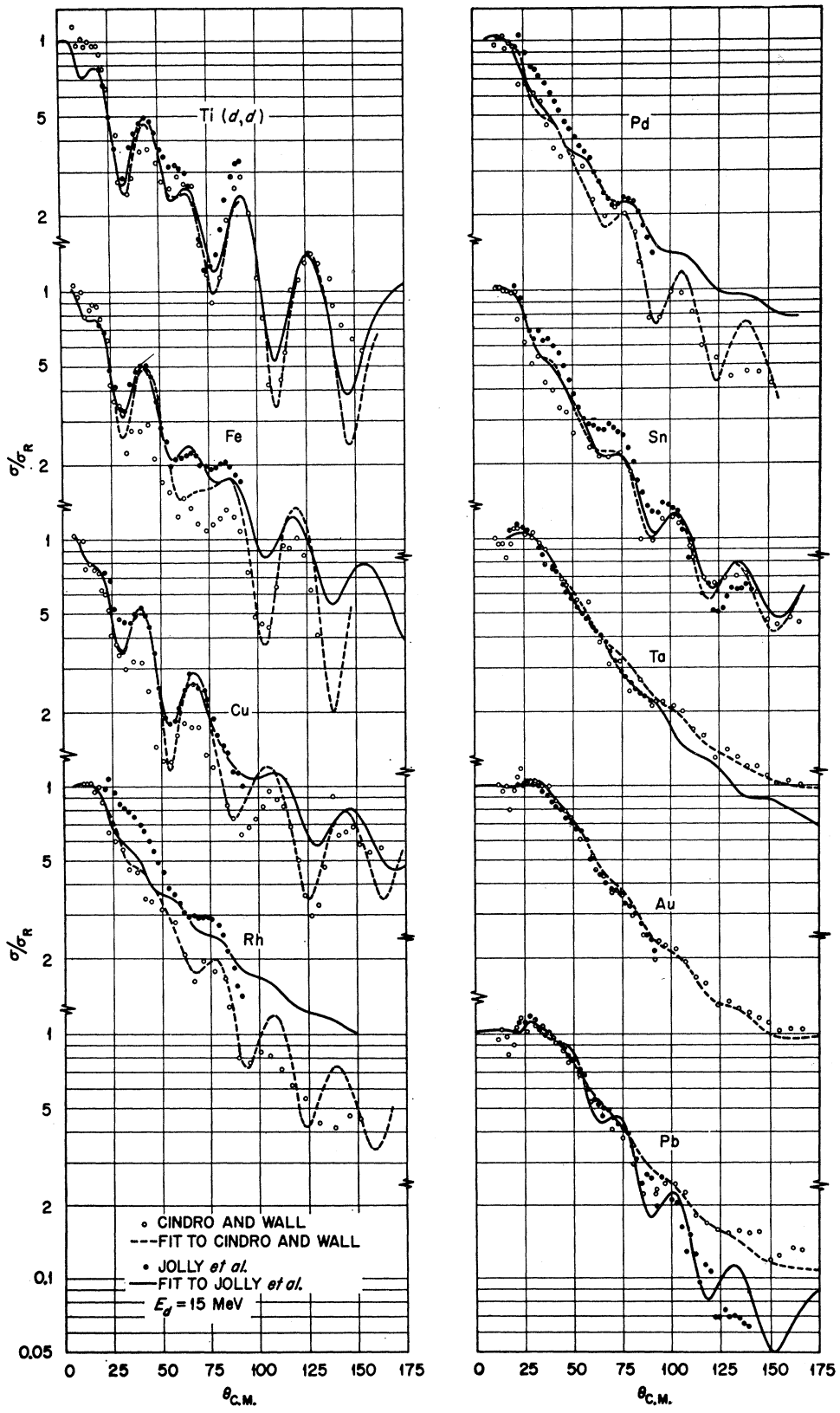

FIG. 5. Comparison of the data of Jolly *et al.* (Ref. 2) and Cindro and Wall (Ref. 3) and curves obtained in fitting each angular distribution by adjusting the two well-depths V_S and W_D for the lowest χ^2 value when the geometrical parameters are kept fixed at the values given in Sec. IV. The numerical values of the well depths are given in Table II.

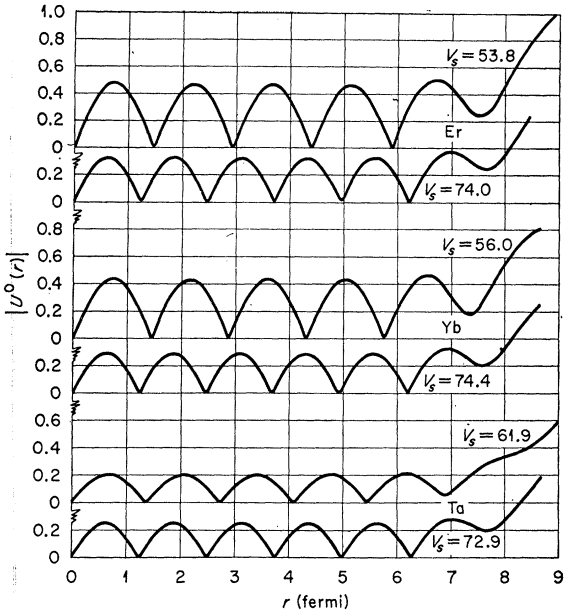

FIG. 6. Moduli of the $l=0$ partial waves as a function of radius for Er, Yb, and Ta. The Er and Yb partial waves were obtained from two different sets of potentials fitting the Jolly *et al.* data. For Ta the first partial wave is obtained from potentials fitting the Cindro and Wall data and the second from potentials fitting the Jolly *et al.* data. The parameters of these potentials are given in Table II.

between the fits for these angles can be explained by the fact that for angles smaller than 50° the calculated differential cross sections are fairly insensitive to the values of V_S and W_D. Therefore the values of V_S and W_D are mostly determined by the data at large angles, particularly when the diffraction patterns are very weak and more pronounced at back angles.

For elements heavier than Sn and a 15-MeV deuteron energy, the diffraction patterns are always very weak and more pronounced at back angles; therefore when large-angle data are available, they greatly influence the optical-model fits for these elements at smaller angles. In the case of Ta, for example, the behavior of the optical-model curve for the Cindro and Wall data at angles less than 90° is determined by the back-angle data. This explains why the fit to the Cindro and Wall data is out of phase with the data of Jolly *et al.*, although, within the considerable scatter of the Cindro and Wall data, the two sets of data themselves appear to agree.

For Pb the disagreement between the two sets of data is greatest for angles larger than 100°, the data differing by as much as a factor of 2. Since the diffraction patterns are approximately in phase, the values of V_S obtained from each set of data are in good agreement, but because of the large amplitude of the oscillations in the data of Jolly *et al.* the value of W_D is half that obtained from the data of Cindro and Wall. A parameter search using the data of Jolly *et al.* for angles smaller than 90° resulted in a value of V_S very close to the previous one and an increase in W_D from 9.5 to 14.8 MeV. The new fit so obtained is shown in the dotted line in Fig. 3.

Anomalies in the Behavior of the Real Well Depths

The obvious departure of some of the real well-depths V_S from the average trend shown in Fig. 4 should be noted. For Al this may be attributed to the fact that we neglect the spin-orbit term, since, as mentioned in paper 1, its effects are fairly large for light nuclei. It was pointed out in paper 1 that the values of V_S for Ni lie below the average values for neighboring nuclei, and this effect is even more pronounced at 15 MeV. There are five other elements for which the values of V_S are significantly different from the average trend: In, Er, and Yb are low by about 7 MeV, and Ta and W are high by 10 and 7 MeV, respectively. The diffraction pattern for In appears to be displaced by a few degrees with respect to those for the two neighboring elements Sn and Cd, and this would account for the low value of V_S; however, from the point of view of nuclear structure there does not seem to be any reason for the displacement. The cases of Er, Yb, Ta, and W are different since they are permanently deformed nuclei, and the "anomalies" for these elements may yield information on the reaction mechansims involved. However, it should be noticed that for these elements the departures from the trend are determined from very small oscillations in the data up to 90°.

In the case of Er and Yb, an attempt was made to find a slightly deeper potential which would fit the data; however, no local minima in χ^2 space were found until the next family of potentials was obtained. The resulting values for V_S and W_D are shown by the solid points on Fig. 4, and the fits to the data are shown by the dotted lines in Fig. 3. The fact that the fits belong to two different families of potentials is illustrated in Fig. 6, where the moduli of the partial-waves $l=0$ are plotted as a function of radius for both potentials. It was shown in paper 1 that a new family of potentials is obtained when the real well depth is increased to the point where the radial wave functions have inside the well exactly one more half wavelength than the preceding family of shallower potentials.

The case for Ta is different. Here the two sets of data are not inconsistent but they yield different values for the real well depths. It appears that the well depth from the Cindro and Wall data is determined mostly by the oscillation in the data at 110°, whereas that from the data of Jolly *et al.* is determined by two weak oscillations which occur in the data up to 90°. The two real well depths differ by 11 MeV. This is not enough to make them belong to two different families of potentials, as can be seen from Fig. 6; therefore it must be concluded that the two sets of data, although in relatively

good agreement, are not consistent with respect to the very weak oscillations in their angular distributions.

VI. CONCLUSIONS

The results of analysis of the new data at 15 MeV are consistent with those discussed in paper 1. The previously observed trend of the parameters to vary smoothly as a function of A was again observed with a few exceptions. We are reluctant to put much weight in the departures of the real well-depth behavior from the trend in some cases, since they resulted from very small oscillations in the data.

PHYSICAL REVIEW VOLUME 134, NUMBER 2B 27 APRIL 1964

Scattering of Polarized 3.25-MeV Neutrons by Medium Weight Nuclei*†

W. P. Bucher‡ and D. W. Kent
Bartol Research Foundation of The Franklin Institute, Swarthmore, Pennsylvania
(Received 6 December 1963)

The polarization produced in the 90° elastic scattering of 3.25-MeV neutrons from Fe, Ni, Co, Cu, Zr, and Mo was measured. The D(d,n)He^3 reaction was used as a source of partially polarized neutrons to determine the scattering asymmetry. The variation of the measured values with the atomic weight indicates a resonance structure similar to that observed by Clement *et al.* at 380 keV but with the polarization ranging from approximately -0.5 to $+0.4$. In addition, polarization measurements of neutrons scattered by C and W were performed.

INTRODUCTION

SYSTEMATIC measurements[1–6] of the elastic scattering of polarized neutrons by medium and heavy weight nuclei have been performed in the 0.4- to 2.1-MeV energy range by several workers for comparison with optical model predictions. Theory is not in good agreement with the results of these experiments. That some disagreement might exist at low energies is not unexpected since fewer levels of both the compound and residual nucleus are involved. The latter condition increases the compound elastic scattering, especially for the lighter of these nuclei.

At higher energies (e.g., 14 MeV) it is possible to fit neutron angular distribution and total cross-section data with a Bjorklund-Fernbach optical-model potential.[7] The inclusion of a spin-orbit coupling term into this potential is necessary in order to yield the correct large-angle scattering. However, the magnitude of this term is not sensitive to the angular distribution and can best be determined by the polarization. This has been shown in the case of 24-MeV neutrons by the work of Wong *et al.*[7] For proton scattering, where many polarization data are available, good agreement is attained[8] for energies above a few MeV.

The neutron polarization data[9–14] for $2.1<E_n<14$

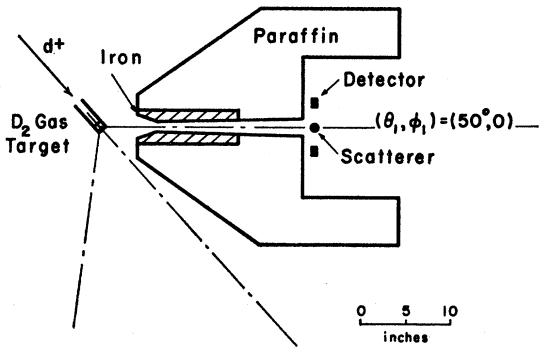

FIG. 1. Experimental arrangement for 90° scattering angle, showing the horizontal cross section view of the collimator.

* Preliminary results of this work have been reported together with later work of D. W. Kent, Bull. Am. Phys. Soc. **7**, 532 (1962).

† Supported by the U. S. Atomic Energy Commission.

‡ Present address: Physikalisches Staatsinstitut, II. Institut für Experimentalphysik, Hamburg, Germany.

[1] R. K. Adair, S. E. Darden, and R. E. Fields, Phys. Rev. **96**, 503 (1954).

[2] A. Okazaki, Phys. Rev. **99**, 55 (1955).

[3] J. D. Clement, F. Boreli, S. E. Darden, W. Haeberli, and H. R. Striebel, Nucl. Phys. **6**, 177 (1958).

[4] L. Cranberg, *Proceedings of the International Symposium on Polarization Phenomena of Nucleons, Basel, 1960*, edited by P. Huber and K. P. Meyer (Berkhauser Verlag, Basel and Stuttgart, 1961), p. 311.

[5] D. Brown, A. T. G. Ferguson, and R. E. White, Nucl. Phys. **25**, 604 (1961).

[6] A. Langsdorf, Jr., A. J. Elwyn, and R. O. Lane, Bull. Am. Phys. Soc. **7**, 532 (1962); D. J. Bredin, Bull. Am. Phys. Soc. **8**, 537 (1963); R. J. Olness, K. K. Seth, and H. W. Lewis, Bull. Am. Phys. Soc. **7**, 576 (1962).

[7] C. Wong, J. D. Anderson, J. W. McClure, and B. D. Walker, Phys. Rev. **128**, 2339 (1962).

[8] F. Bjorklund, G. Campbell, and S. Fernbach (see Ref. 4, p. 432).

[9] P. S. Ot-Stavnov and V. I. Popov, Zh. Eksperim. i Teor. Fiz. **43**, 385 (1962) [English transl.: Soviet Phys.—JETP **16**, 276 (1963)].

[10] A. E. Remund, Helv. Phys. Acta **29**, 545 (1956).

[11] B. M. McCormac, M. F. Steuer, C. D. Bond, and F. L. Hereford, Phys. Rev. **108**, 116 (1957).

[12] F. L. Hereford (see Ref. 4, p. 303).

[13] K. V. K. Iyengar and R. A. Peck, Jr., Phys. Rev. **125**, 1000 (1962).

[14] J. Durisch, R. Gleyvod, P. Huber, and E. Baumgartner, Helv. Phys. Acta **36**, 269 (1963).